# EU Contribution to the Test and Analysis of the ITER Poloidal Field Conductor Insert (PFCI)

R. Zanino 1), M. Bagnasco 2), D. Ciazynski 3), B. Lacroix 3), E.P.A. van Lanen 4), A. Nijhuis 4), L. Savoldi Richard 1), C. Sborchia 5), A. Vostner 5)

1) Dipartimento di Energetica, Politecnico di Torino, Italy
2) EPFL-CRPP, Villigen PSI, Switzerland
3) CEA, IRFM, F-13108 Saint-Paul-lez-Durance, France.
4) University of Twente, The Netherlands
5) F4E Barcelona, Spain

e-mail contact of main author: roberto.zanino@polito.it

**Abstract**. The PFCI is a single-layer solenoid wound from a 45 m long ITER-type NbTi dual channel cable-in-conduit conductor, designed to be representative of the one currently proposed for the ITER PF1&6 coils. The PFCI, installed in the bore of the ITER Central Solenoid Model Coil at JAEA Naka, Japan, and well instrumented from both the thermal-hydraulic and the electromagnetic points of view, has been successfully tested in June-August 2008. The test concentrated on: DC performance (current sharing temperature and critical current measurements), AC loss measurements, stability and quench propagation. The preliminary results of the analysis of the PFCI test are reported in the paper, with emphasis on DC performance and AC losses and particular attention to the comparison with the short sample which was previously tested in the SULTAN facility.

## 1. Introduction

The PFCI is the last in a series of Model and Insert Coils tested within the ITER R&D framework from year 2000 on [1-5], and the first one using NbTi. Because of their operation in low magnetic field (≤ 6 T), the ITER Poloidal Field (PF) coils will make use of NbTi as superconductor, in order to reduce the cost of fabrication. The PFCI is a single-layer solenoid, see Fig. 1a, wound from a 45 m long ITER-type NbTi dual channel Cable-In-Conduit Conductor (CICC), see Fig. 1b. An Intermediate Joint (IJ) connects the main winding to a second piece of the same conductor, which is called the upper busbar, see Fig. 1a. The conductor is representative of the one currently proposed for the ITER PF1&6 coils [6]. The IJ was included in the winding in order to test an ITER relevant joint under the PF operating conditions (i.e. axial and radial magnetic field variations). The PFCI main winding and upper busbar are cooled by two separate hydraulic circuits using supercritical helium at nominal 4.5 K and 0.5 MPa inlet conditions.

The PFCI was fabricated by Tesla Engineering, UK, starting from a cable produced in Russia by VNIIM/VNIIKP and jacketed at Ansaldo Superconduttori, Italy [7]. Like its predecessors, it was installed in the bore of the ITER Central Solenoid Model Coil (CSMC) at JAEA Naka, Japan [8], see Fig. 1c. The PFCI is well instrumented both from the thermal-hydraulic point of view, with thermometers along the conductor, flow meters, pressure taps and different heaters on inlet piping, conductor and IJ, see Fig. 1a, and from the electromagnetic point of view, with a series of voltage taps located along and around the main winding, together with pick-up (PU) coils, close to the main winding and IJ, for magnetization measurements [9]. The CSMC provides the nominal background field of 6 T, whereas the nominal operating current of 45 kA adds a non-negligible self-field contribution, leading to a significant field variation (~ 1 T) over the cross section of the conductor, similar to that in the ITER PF coils.

The PFCI was tested during about two months until mid-August this year and the main test results are summarized in [6]. This paper will concentrate on the preliminary analysis of the two major items of the test, namely

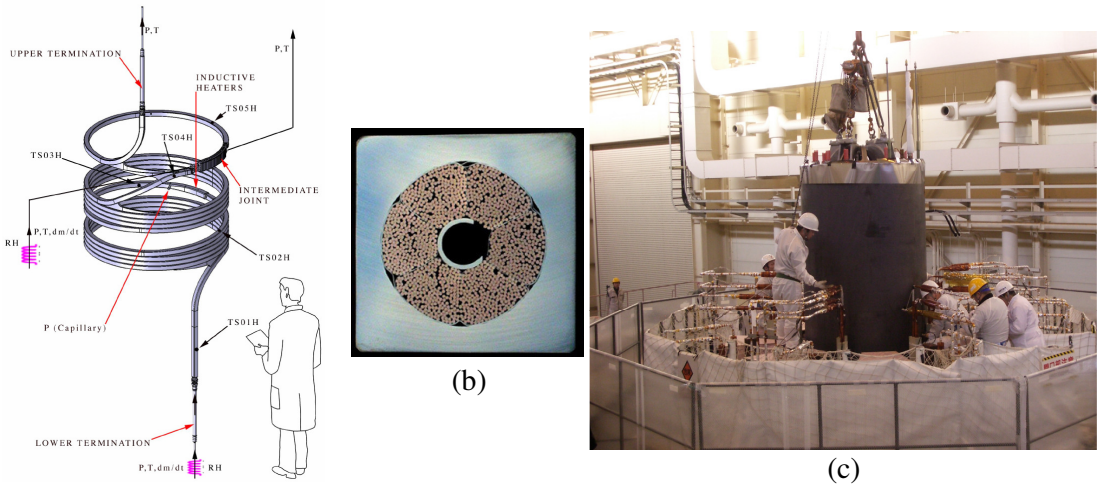


*FIG. 1 (a) Sketch of the PFCI with some instrumentation. (b) Cross section of the PFCI CICC (square SS jacket side ~ 50.3 mm). (c) The PFCI being inserted in the CSMC bore at JAEA Naka, early 2008.*

- Current sharing temperature ($T_{CS}$) and critical current ($I_C$) measurements;
- AC loss measurements in the main winding and in the IJ;

based on the analysis work performed on these items so far in the different EU laboratories. Some emphasis will also be put on the validation of the models and on the verification of their *predictive* capabilities, based on some exercises performed before the tests [10].

The results of the PFCI test improved on the reduced performance shown by the PFCI short sample [11, 12], tested in 2004 in the SULTAN facility at Villigen PSI, Switzerland, and more generally provide a significant database for the ITER PF coils. In particular, the tests confirmed that:

- While sudden quenches still occur above a certain current threshold, because of (self-field) gradient on the CICC cross section, the PFCI could operate in DC conditions with no premature quenches with respect to its strand at peak magnetic field, as opposed to the case of the short sample – an indirect indication of improved current uniformity. Some degradation was observed, however, at the maximum ramp-rate allowed by the test setup [6].
- The resistance of the IJ (and lower termination) was much lower than in the case of the short sample thanks to improved manufacturing: $R_{IJ}$ [nΩ] = 2.03 +0.057*$B_{IJ}$ [T] ± 0.14 was measured electrically [6] and confirmed calorimetrically – calorimetry also attributed up to 60% of the resistance to the side of the joint feeding the upper busbar and the remaining 40% to the side of the main winding. However, the performance of the joint itself was degraded with respect to the conductor [6].
- The AC losses in the PFCI main winding follow the similar trend with cycling as measured on the Twente press.

## 2. DC Performance

The results of both $T_{CS}$ and $I_C$ tests of the PFCI (undistinguished, since they lead to essentially identical results) are summarized in Fig. 2, where they are reported in the form of relative deviation with respect to the collective strand-like behavior at peak magnetic field, i.e., with respect to [$I_C^{strand}$ ($B_{peak}$) * (# of strands)], and compared with the short sample results. All results are given as a function of measured (jacket) temperature in the high field region, and

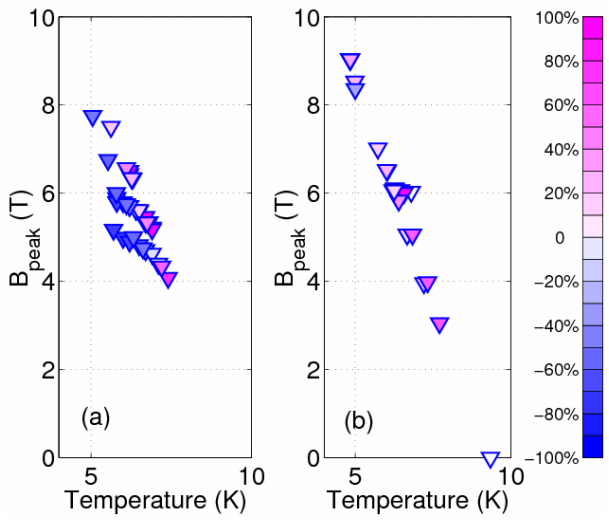


*FIG. 2. Summary of DC performance results compared with $I_C$ at $B_{peak}$ from strand: short sample (a), PFCI (b). The relative deviation (dimensionless) between the measured critical or quench current and that resulting from all strands carrying the $I_C$ at peak field is reported*

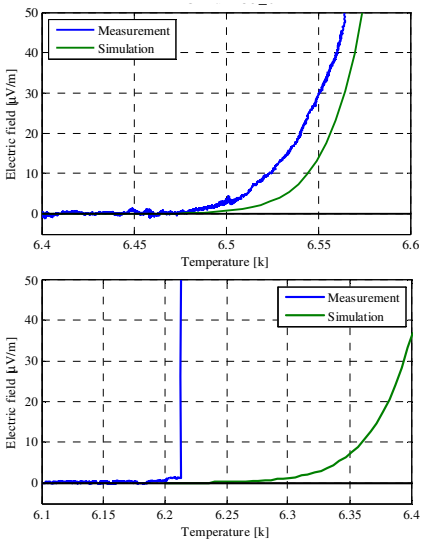


*FIG. 3. Evolution of measured and computed (JackPot) voltage in the case of two $T_{CS}$ tests, based on the T03H signal: run 53-01, $I_{PFCI}$ = 6 kA and $B_{CSMC}$ =5.9 T (top), run 35-01, $I_{PFCI}$ = 45 kA and $B_{CSMC}$ = 5.15 T (bottom).*

*peak* magnetic field. We see that the PFCI results typically correspond to and sometimes even somewhat outperform the strand at peak magnetic field (large positive deviations are partly an artifact of a small denominator in case of small currents) as opposed to the short sample, where also significant negative deviations are noted. Both the PFCI and the short sample exhibit limiting currents, above which no critical current strictly speaking can be measured, but their performance is different above this limiting current.

In the PFCI $T_{CS}$ and $I_C$ tests, both smooth and sudden transitions occurred depending on the current level: as an example, it can be seen in Fig. 3 that the transition was smooth at "low" current but sudden at "high" current, which is a common feature of both the PFCI and the short sample [11, 13] (of course, the strand itself is stable at the peak field value, when tested on a barrel). Both the strand-like performance (in case of uniform current distribution) and the smooth vs. sudden transition at low vs. high currents were anticipated by the predictive simulations [10].

The recently developed model JackPot [14], accounting for the precise strand trajectories in the spatial varying magnetic field, substantiates why there can be an important difference in performance between the test of a short sample and a coil, in particular for high currents. The model demonstrates that the disturbing influence of the joints on the PFCI test results, as observed in earlier tests on a short sample of a similar PF cable, attributed to a combination of non-uniformity and local peak voltages [11], is practically negligible. A good assessment of the coil requires a priori the ability for sufficiently homogeneous current distribution among the strands in the high field region, and this condition is reached in the PFCI, see [14]. Only near the joints, the current distribution remains inhomogeneous beyond this level, but since the magnetic field in this region is sufficiently low, this does not affect the performance. The relatively large non-uniformity in the short sample test is confirmed by transverse voltage measurements and Hall sensor array analysis [15]. Two $T_{CS}$ runs (35-1 and 53-1) were simulated with JackPot and compared with the signal from VD_0910, see Fig. 3, against the temperature measured at T03H with correction for magnetic field dependency (see Appendix). The results show that for the run with lower current the test result is only 0.02 K lower than

the simulation. For the high current run the measured $T_{CS}$ is 0.14 K below that from the simulation.
A different approach can be followed by computing the average electric field across the cable cross-section using the magnetic field map (uniform field gradient assumed), the measured strand critical current and n value [16] and assuming a uniform current distribution among all strands. Two runs (25-1 and 45-1) have been checked, one at high current (45 kA) and the other at low current (18 kA). The $T_{CS}$ then computed (regardless of a possible instable behavior) is ~ 6.4 K and ~ 6.5 K, respectively, which is within 0.1 K from measured. These deviations should be considered with regard to possible slight current distribution imbalance, temperature gradients (ignored in the model) and thermometer accuracy. The major conclusion here is that if we compute $T_{CS}$ for uniform current we should find a somewhat higher $T_{CS}$ than strand at peak field and therefore higher than in the experiment (e.g., due to current non-uniformity).

## 3. AC Losses

AC losses were measured on both the conductor and the IJ using different test scenarios (exponential, trapezoidal, etc.) as well as in different phases of the tests (i.e., before, during and after completing a series of about 9000 full loading cycles) [6]. The major outcome of the conductor measurement is the characteristic coupling time constant "$n\tau$", to be compared with the measurement results on a PFCI conductor short sample in the Twente press [17] and on sub-size NbTi conductors in SULTAN [18]. The AC loss measured in the Twente press showed an initial decrease from the virgin state value (~ 15 ms) down to ~ 10 ms, followed then by a monotonic increase to ~ 30 ms after 10000 cycles and ~ 50 ms after 40000 cycles (exact values depending also on the load conditions). As opposed to this, an earlier saturation of the loss was observed in SULTAN tests of sub-size NbTi samples. Below we describe the present status of our analysis of the PFCI losses.

### 3.1 Calorimetric evaluation of conductor and IJ losses

The assessment of the AC loss is in principle straightforward, but very delicate in practice, see below. With reference to Fig. 4 we may note that steady state 0D energy balances can be written separately for main winding, IJ and upper busbar, respectively, as follows:

$$Q_{WIND} = (dm/dt)_{cond} * [h(p,T04H) - h(p,TCin)]$$
$$Q_{IJ} = (dm/dt)_{cond} * [h(p,TCout) - h(p,T04H)] + (dm/dt)_{bus} * [h(p,T05H) - h(p,TIJin)]$$
$$Q_{BUS} = (dm/dt)_{bus} * [h(p,TIJout) - h(p,T05H)] + (dm/dt)_{IPI} * [h(p,T06H) - h(p,TCin)]$$

where the single terms have the dimensions of a power (W), dm/dt is the mass flow rate, h is the helium enthalpy, p the pressure, all functions of time as measured. $Q_{WIND}$ strictly speaking includes the loss in the lower termination, but this is considered negligible in view of the very low field there ($B^2/B_{peak}^2 < 0.1$). The total (hysteresis + coupling) energy loss (J) of the main winding conductor can then be obtained by integrating $Q_{WIND}$ in time (a similar integration will give the energy loss of the other components, as well as the total).
The major difficulty and uncertainty involved in this exercise is a consequence of some details in the temperature evolution measured on the conductor at T04H and may be explained by considering, as an example representative of the situation typical of most CSMC exponential dumps, Fig. 5 below. It can be seen that:

1) Initial values of $T04^{corr}$ and $T05^{corr}$ (see Appendix) are lower than the respective inlet temperatures by 75 mK and 90 mK and $T04^{corr}$ is anyway outside the range [$TC_{in}$, $TC_{out}$], which is finite because of the Joule-Thompson effect

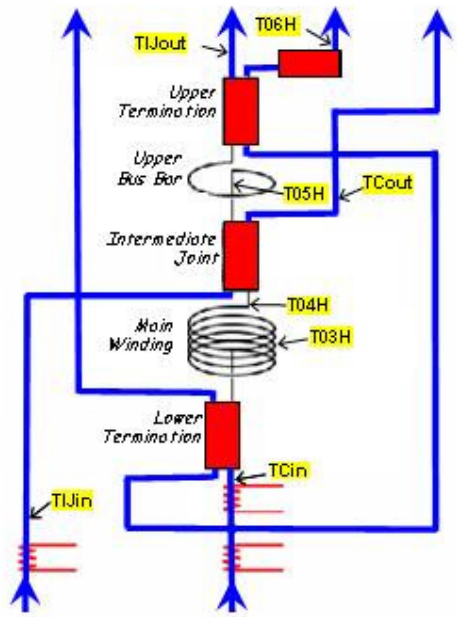


*FIG. 4. Sketch of the hydraulic circuits relevant for PFCI calorimetry.*

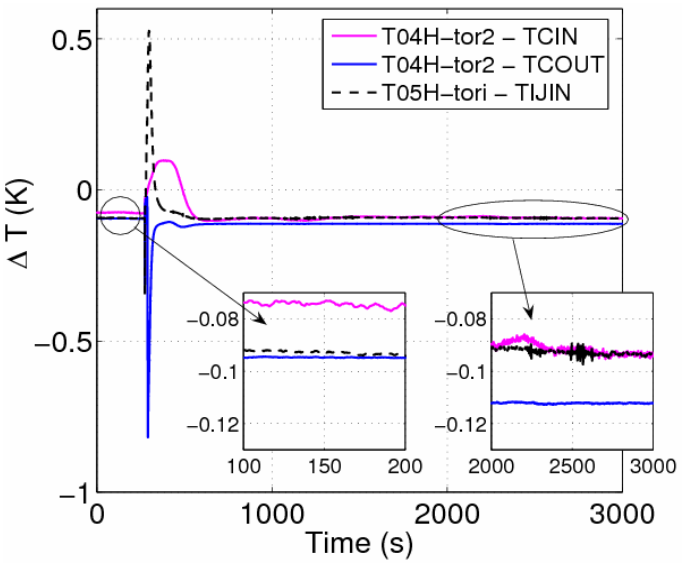


*FIG. 5. Evolution of measured (corrected) temperature differences of relevance for the calorimetric assessment of AC losses. Case of run 74-02.*

2) While the final value of $T05^{corr}$ returns more or less to the initial value, $T04^{corr}$ returns at the end of the transient to a value which is ~ 20 mK below the initial one.

To address these issues we adopted two different strategies: a) offset the already corrected temperatures with respect to their *initial* value. This leaves an arbitrariness in the final integration time, which has to be chosen "as early as possible" (compatibly with a reasonable steady state), to limit the cumulative error on the computed energy; b) offset the already corrected temperatures with respect to their *final* value (note that initial and final values are affected by the different magnetic field). The two results are then used to provide some sort of effective error bar.

The calorimetric estimates of the AC loss for the reference CSMC exponential dumps from 4T ($\tau_{dump}$ ~ 5.6 s), with $I_{PFCI}$ = 0 kA, are presented in Table I. In order to separate coupling and hysteresis losses the model presented in [19] based on classical formulas was used. It turns out that the hysteretic contribution is ~ 250 J roughly independent of cycling.

It is seen that the conductor losses increase with cycling until quench events bring the conductor back or close to virgin values, but then values close to those before quench are

TABLE I: AC LOSSES IN CSMC EXP DUMPS FROM 4 T ($\tau_{dump}$ ~ 5.6 s, $I_{PFCI}$ = 0 kA).

| **Run #** | **Cycles** | **$E_{cond}$ (J)** | **$E_{IJ}$ (J)** | **$M_{IJ\text{-}axial}$ (a.u.)** | **$M_{IJ\text{-}radial}$ (a.u.)** | **$E_{tot}$ (J)** | **nτ (ms)** |
|---|---|---|---|---|---|---|---|
| 54-2 | Before cyclic test | 1167/1437 * | 2012/1635 * | 16.5 | 9.22 | 3242 | 34 - 44 * |
| 63-2 | ~ 430 | 1455/1955 * | 2537/1963 * | 16.2 | 9.63 | 4136 | 45 - 64 * |
| 66-2 | ~ 1000 | 1742 | 2459 | | | 4367 | 56 |
| 69-2 | ~ 1700 | 2016 | 2334 | | | 4546 | 65 |
| 71-2 | ~ 2800 | 2293 | 2326 | | 9.82 | 4761 | 76 |
| 74-2 | ~ 4000 Before quench test | 2173/2652 * | 2454/1869 * | | 10.03 | 4741 | 72 - 90 * |
| 119-2 | After quench test | 1199/1199 * | 1976/1760 * | | | 3282/3165 * | 35 |
| 134-2 | ~ 9000 Before high-field quenches | 1428/3111 * | 3406/2057 * | | | 5011/5447 * | 44 - 107 * |

* offset correction at final time

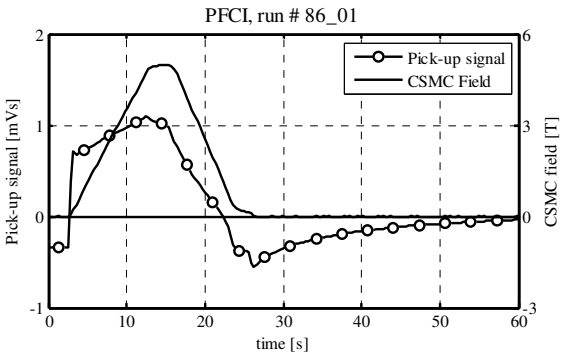


*FIG 6. Time-integrated pick-up signal and trapezoidal CSMC field pulse.*

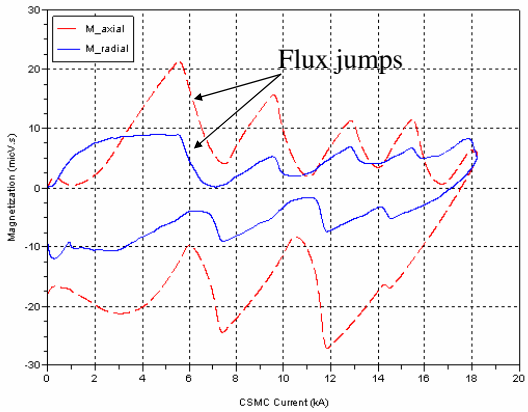


*FIG 7. PU Magnetization loops (radial and axial directions) of the IJ during a CSMC trapezoidal field pulse at 18.2 kA.*

being recovered again after further cycling.
However, a rather significant uncertainty is present in the calorimetric estimates for most runs, which should be improved in future work. This is important particularly in view of the fact that the most pessimistic estimate at the end of the cycles hits the 100 ms ceiling, which defines the acceptable upper bound for ITER PF coils. Finally, it should be noted that there is some disagreement, although within the present (large) error bars of the calorimetric assessment, in the strong variation of IJ AC losses from virgin to cycled, with respect to the magnetization estimates, see below.

**3.2 Evaluation of conductor and IJ losses from magnetization measurement (PU coils)**
The signal from the conductor PU coil may be useful for confirmation of the conductor magnetization and thus the conductor AC losses in terms of coupling and hysteresis components. For the coupling loss, the multiple time constants nature [20] associated with the complex cabling pattern in large CICCs is clearly illustrated by the long decay time of the coupling currents at the end of a trapezoidal run. In Fig. 6 the PU signals from sensor IPF_VC_01 (middle of winding) and the CSMC field are plotted versus time. When the CSMC trapezoidal field pulse is completed, there is still a significant decay of the magnetisation, indicating decay of coupling currents associated with large loops. A similar decay occurs at the end of the rise of the field but the plateau is too short for full relaxation. The low pass filtering of the PU coil signals by the PFCI instrumentation is probably too severe for the higher harmonics to allow detection of the short time constants of around several tens of ms, expected to be the most dominant ones from the calorimetric assessment above. A simple two time constant fit to the decaying signal after the field pulse gives time constants of about 2 s and about 12 s.
The plots in Fig. 7 show the IJ magnetization according to the axial and radial field directions (with respect to the coil) during a CSMC trapezoidal field run: the axial field amplitude is 3.6 T and the radial field amplitude is 1.2 T, the ramping up and down times are both equal to 17 s. Note that the values at maximum current are unsure because of a too short plateau duration (≈ 3 s) to allow a full relaxation of the induced currents. One can clearly see in this figure a series of so-called “flux-jumps” i.e. fast decreases of the magnetization which correspond to overload and local quench of strands inside the joint due to high screening currents induced by the field change in the joint. This phenomenon was anticipated from measurements performed on sub-size joints and PU coils were used to diagnose these instabilities, which cannot be identified by calorimetry because of the too short time scale of these sudden events; then only a decrease of the losses when increasing the ramp rate can be measured [21].

Although the modeling has not yet been achieved to be able to compute directly the energy loss from the areas of the magnetization curves, the proportionality of these areas with the energy loss already allows relative estimations between runs (see Table I), to be compared with the calorimetric estimates.

## 4. Conclusions and Perspective

- The good overall results of the PFCI conductor DC tests are being interpreted by the models and the improvement with respect to the short sample is explained by improved uniformity of the current.
- Calorimetric analysis of AC losses qualitatively confirms the trends of conductor $n\tau$ with cycling as observed on the Twente press, but error bars are still large at present for the PFCI.
- The analysis of stability and quench is ongoing and shall be presented elsewhere.
- RRL and joint degradation remain open issues for the analysis.

## 5. Acknowledgments

The participation of RZ, BL, LSR, AV to the PFCI test was financially supported by EURATOM mobility. The kind hospitality of JAEA Naka, Japan, during the test period is also gratefully acknowledged. The work of RZ and LSR was also partially financially supported by the Italian Ministry for University and Research (MiUR) and LSR is a grateful recipient of a fellowship "Giovani ricercatori" of Politecnico di Torino. EPAvL is partially financially supported by the University of Twente. MB is partially financially supported by CRPP. Both MB and EPAvL were also supported by a Marie Curie trainee fellowship. Thanks to L. Zani, A. Torre, and S. Nicollet (all from CEA) for their contribution to the analysis work. This report was prepared as an account of work for the ITER Organization. The Members of the Organization are the People's Republic of China, the European Atomic Energy Community, the Republic of India, Japan, the Republic of Korea, the Russian Federation, and the United States of America. The views and opinions expressed herein do not necessarily reflect those of the Members or any agency thereof. Dissemination of the information in this paper is governed by the applicable terms of the ITER Joint Implementation Agreement.

## 6. Appendix: PFCI Thermometry

Of the originally five thermometers installed on the conductor (four of which – TS01H-TS04H -- on the main winding, the last one – TS05H – on the upper busbar, see [9]) only three (TS03H-TS05H) survived at the time of the test. However, also these thermometers did not show a very accurate reading and had to be recalibrated in situ. We give below the result of the recalibration, which allows converting from raw data, as available on the web, to the values used for the assessments presented in this paper, at different magnetic field (resulting from different CSMC currents, $I_{CSMC}$, while the contribution of the PFCI current is neglected in this parameterization). Note that also these corrected values are available on the web, from the list of virtual sensors, under the names TS03H_Tor2, TS04H_Tor2, TS05H_Tori. For TS03H and TS04H, the corrections are in the form:

$TS0xH^{corr} = y0x * (1 - I_{CSMC}[kA]/20) + y1x * I_{CSMC}[kA]/20$

y03 = 1.1527 * TS03H – 0.4322, y13 = 1.1582 * TS03H – 0.3932 (between 4.5 K and 6.8 K)

y04 = 1.5422 * TS04H – 0.9793, y14 = 1.5328 * TS04H – 0.9069 (between 4.5 K and 6.8 K)

while for TS05H the field dependence of the correction appears negligible and we have:

$TS05H^{corr}$ = 2.5887 * TS05H – 2.3011 (between 5.3 K and 6.8 K)

Note that these corrections are not simple offsets, i.e., not even the temperature differences are reliable in the raw data.

## 7. References

[1] TSUJI, H., et al., "Progress of the ITER Central Solenoid Model Coil Program", Nucl. Fusion **41** (2001) 645.
[2] MARTOVETSKY, N., et al., "Test of the ITER Central Solenoid Model Coil and CS Insert", IEEE Trans. Appl. Supercond. **12** (2002) 600.
[3] ULBRICHT, A., et al., "The ITER Toroidal Field Model Coil Project", Fus. Eng. Des. **73** (2005) 189.
[4] OKUNO, K., et al., "Test of the NbAl Insert and ITER Central Solenoid Model Coil", IEEE Trans. Appl. Supercond. **13** (2003) 1437.
[5] MARTOVETSKY, N., et al., "Test of the ITER TF Insert and Central Solenoid Model Coil", IEEE Trans. Appl. Supercond. **13** (2003) 1441.
[6] BESSETTE, D., et al., "Test results from the PF Conductor Insert Coil and implications for the ITER PF system", presented at ASC, Chicago (IL) USA, August 2008.
[7] BAKER, W., et al., "Manufacture of the poloidal field conductor insert coil (PFCI)", Fus. Eng. Des., **82** (2007) 1567.
[8] NUNOYA, Y., et al., "Installation and Test Programme of the ITER Poloidal Field Conductor Insert (PFCI) in the ITER Test Facility at JAEA Naka", presented at ASC, Chicago (IL) USA, August 2008.
[9] ZANINO, R., et al., "Preparation of the ITER Poloidal Field Conductor Insert (PFCI) Test", IEEE Trans. Appl. Supercond. **15** (2005) 1346.
[10] ZANINO, R., et al., "Predictive Analysis of the ITER Poloidal Field Conductor Insert (PFCI) Test Program", IEEE Trans. Appl. Supercond., **17** (2007) 1353.
[11] BRUZZONE, P., et al., "Test Results of the ITER PF Insert Conductor Short Sample in SULTAN", IEEE Trans. Appl. Supercond., **15** (2005) 1351.
[12] ZANINO, R., et al., "Implications of NbTi Short-Sample Test Results and Analysis for the ITER Poloidal Field Conductor Insert (PFCI)", IEEE Trans. Appl. Supercond., **16** (2006) 886.
[13] CIAZYNSKI D., et al, "DC Performances of ITER NbTi Conductors: Models vs. Measurements", IEEE Trans. on Applied Superconductivity, June 2005, vol. 15, Nr. 2, 1355.
[14] VAN LANEN, E.P.A., et al.,"Simulation of the ITER Poloidal Field Coil Insert DC Performance with a New Model", presented at SOFT 25, Rostock, Germany, September 2008.
[15] ILYIN, Y, et al., "Interpretation of conduit voltage measurements on the Poloidal Field Insert Sample using the CUDI-CICC numerical code", Cryogenics **46** (2006) 517.
[16] ZANI L., et al., "Jc(T,B) Characterization of NbTi Strands Used in ITER PF-Relevant Insert and Full-Scale Sample", IEEE Trans. Appl. Supercond. **15** (2006) 3506.
[17] ILYIN, Y., et al, "Effect of Cyclic Loading and Conductor Layout on Contact Resistance of Full-Size ITER PFCI Conductors", IEEE Trans. Appl. Supercond. **15** (2005) 1359.
[18] BRUZZONE, P., et al., "A Critical Review of Coupling Loss Results for Cable-in-Conduit Conductors", IEEE Trans. Appl. Supercond. **16** (2006) 827.
[19] LACROIX, B., et al., "Predictive study of the Poloidal Field Coil Insert behaviour under pulsed current tests", presented at EUCAS (2007).
[20] NIJHUIS, A, et al, "Study on the coupling loss time constants in full size Nb3Sn CIC model conductors for fusion magnets" Adv. Cryo. Eng. **42B** (1995) 1281.
[21] ZANI, L., et al., "Manufacture and Test of NbTi subsize Joint Samples for the ITER Poloidal Field Coils", IEEE Trans. Appl. Supercond., **13** (2003) 1460.